SAND2017-6069C

A Predictive Engine for On-Line Optimal Microgrid Control

Joseph Young
OptimoJoe
Albuquerque, NM
Email: joe@optimojoe.com

Marvin A. Cook
Military and Energy Systems Analysis
Sandia National Laboratories
Albuquerque, NM
Email: macook@sandia.gov

David G. Wilson
Electrical Science and Experiments
Sandia National Laboratories
Albuquerque, NM
Email: dwilso@sandia.gov

***Abstract*—This research presents a predictive engine that integrates into an on-line optimal control planner for electrical microgrids. This controller models the behavior of the underlying system over a specified time horizon and then solves for a control over this period. In an electrical microgrid, such predictions are challenging to obtain in the presence of errors in the sensor information. The likelihood of instrumentation errors increases as microgrids become more complex and cyber threats more common. In order to overcome these difficulties, details are provided about a predictive engine robust to errors.**

I. Introduction

Before the impact of inaccurate or misleading information on the optimal control engine can be considered, the control algorithm in question must be specified and fixed. This paper considers a controller that uses an optimal control algorithm based on an on-line optimization engine with a receding-horizon control. Each of these components is considered in turn.

In the following discussion, the control engine employed uses an optimal control formulation detailed in the documents by Wilson et al. [1], [2]. Specifically, the term *optimal control* is used because this control is based on an optimization formulation that attempts to minimize a specified criteria. Given that the formulation is not convex, the control engine can not guarantee a global minima, but given enough time, it can guarantee at least a local minima.

In order to specify this optimization problem, the microgrid is modeled as a circuit using Kirchhoff's circuit laws. In this model, power generation is represented as either a current or voltage source and the power/energy storage device is represented similarly. Next, the circuit equations are solved while optimizing a user specified metric such as minimizing the use of the storage devices or minimizing the change in the boost converter duty cycles. In addition to this optimization, the behavior of the grid is constrained by requiring certain quantities such as the current or voltage of certain components to remain within specified amounts. For example, a high-level overview of one such formulation can be found in Table I with the components A, B, and C described in Figures 1, 2, and 3.

Since the optimal control problem above is highly nonlinear, a hard guarantee on how long it takes for the optimizer to solve the formulation can not be provided. Generally, this guarantee of performance can only be provided by a linear-quadratic control, which consist of a quadratic objective function with linear equality constraints and no bounds. When the control has a quadratic objective and linear equality constraints, the first-order optimality conditions consist of a single linear system that must be solved. If a direct method is used to solve this system such as Gaussian elimination or preferably a factorization such as an LU or a symmetric indefinite factorization, the number of FLOPS required to find a solution can be counted, which provides a real-time guarantee. In the case of a nonlinear, nonconvex optimization formulation, an appropriately designed algorithm based on line-search or trust-region methodology can guarantee that a solution can be found in a finite number of optimization steps. Though, it is unknown how many steps may be required.

Minimize	Use of storage devices
Subject to	Boost converter state equations (A)
	DC bus state equations (B)
	DC to DC bus state equations (C)
	Power and energy equations
	ODE discretization
	Bounds on voltages, currents, duty cycles, etc.

TABLE I. Optimal control formulation

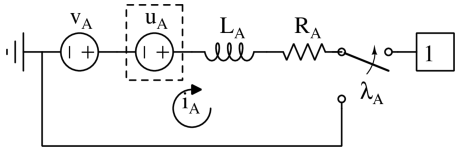

Fig. 1. Boost converter (A)

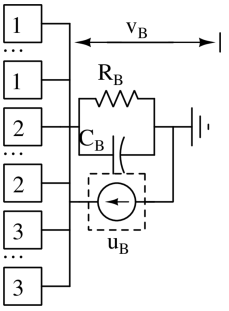

Fig. 2. DC bus (B)

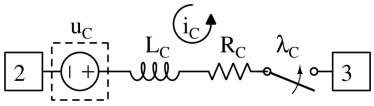

Fig. 3. Connector between DC buses (C)

Therefore, a control algorithm based on the above optimization formulation is not a real-time controller. Practically speaking, one can get a feeling of how long it takes to solve a particular formulation with a fixed size, but this does not provide any guarantee on the performance of the control.

Although this controller provides no real-time guarantees, it may still be used in an on-line control. An *on-line control* repeatedly solves the control problem on a system in operation over a specified time horizon. This differs from an *off-line control* that solves the control problem a priori for a system not currently in operation. The key behind an on-line controller is that although the state of the system depends on a collection of unknown inputs, if the behavior of the system can be predicted well enough over the time horizon, it can provide a useful control.

In order to make this process of prediction and control more robust, this controller uses a *receding-horizon control*, which is also known as a *model-predictive control*. In a receding-horizon control, the behavior of the system is predicted over a specified time horizon and then a control over this time period is determined. This is called the *planning horizon*. If the state of the system diverges too far from this prediction, the current plan is abandoned and a new control is solved for. This shorter time window is called the *execution horizon*.

As an important note, given that an on-line control does not have run-time guarantees, such controller is typically used as a high-level control for long-term planning. For short-term plans, one typically needs to combine the on-line control with a real-time control that moderates rapidly changing dynamics in the system. Although the performance of the real-time controller is critical to the performance of the system, this paper focuses on the longer term on-line control.

For an optimal microgrid control, an energy management layer would incorporate both a priori information and real time instrumentation. In this context, the energy management layer must specify the control problem based on control objectives and measured values, then evaluate the accuracy of the returned solution. By monitoring measurement signals during execution, the energy management layer determines when to recalculate solutions and adjust the planning horizon.

Historically, optimal control algorithms based on on-line optimization engines have been used for decades within the chemical engineering community. For example, Jang et al. discuss on-line controls applied to chemical processes [3]. In addition, Biegler discusses more recent results in the application of nonlinear model predictive controls applied to the chemical industry [4]. This paper differs from these results by applying these control techniques to a different problem area, electric ships, and it explores a different method for predicting the behavior of the system.

In the realm of electric ships, Park et al. explored the use of a model predictive control for shipboard power management systems [5]. There, the authors utilize an integrated perturbation analysis and sequential quadratic programming (IPA-SQP) solver [6] to find controls that dictate how power is used within the system. This is similar to the work by Wilson et al. [1], [2], which uses an SQP algorithm to find an on-line optimal control. These two groups differ in that Park et al. attempt to find a real-time controller, but sacrifice optimality in the case where the perturbation in the initial conditions is too large. The controller from Wilson et al. retains optimality, but this controller provides no real-time guarantee and must be used on-line. Each group also bases their controller on a different model of the power system. This paper differs from these results by exploring a method for predicting the behavior of the power system and how that affects the control.

Aggregating the above, this paper considers a controller that implements an optimal control algorithm based on an on-line optimization engine that uses a receding-horizon control. Absent errors in the optimization algorithms that implement the control, the performance of the controller depends directly on the predictive engine used to predict the behavior of the system. Therefore, it is important to assess the impact of inaccuracies or errors in the information provided to the predictive engine. These errors can arise from either mundane causes such as instrumentation errors or more malevolent causes such as cyber attacks.

II. Predictive Engine

In order to build a predictive engine, it is assumed that one knows the overall shape of the signal to predict, but not how it's scaled or time delayed. To that end, let $\phi : \mathbb{R} \to \mathbb{R}$ be the known signal and consider three modifications of the function

- Time shift - $\phi(t - T)$
- Time scaling - $\phi(\alpha t)$
- Amplitude scaling - $\beta\phi(t)$

Combining each of these produces an adaptable signal of the form

$$\beta\phi(\alpha t - T). \tag{1}$$

It can be observed that the adaptable signal allows one to adjust and match the actual signal in three different ways, but it does not allow adaptation to an arbitrary signal. That's the penalty one must pay for predicting the future.

In order to match the adaptable signal to data, $\{(t_i, y_i)\}_{i=1}^m$, the following optimization problem is solved

$$\min_{(T,\alpha,\beta)\in\mathbb{R}^3} \sum_{i=1}^{m} (\beta\phi(\alpha t_i - T) - y_i)^2. \tag{2}$$

Note, the above prediction engine requires knowledge of what signal is to be adapted a priori. This prediction can be extended to a finite number of signals in the following manner. Let $\{\phi_j\}_{j=1}^n$ be a collection of known signals. Then, the optimization problem

$$\min_{j=1,\ldots,n} \left\{ \min_{(T,\alpha,\beta)\in\mathbb{R}^3} \sum_{i=1}^{m} (\beta\phi_j(\alpha t_i - T) - y_i)^2 \right\} \tag{3}$$

can be solved to identify the signal with the best match. In other words, each signal in the collection is matched to the data and the one with the best match is chosen as the prediction.

III. Results

In the following section, a series of numerical experiments are presented to quantify the robustness of the predictive engine and control to errors from the sensors.

A. Prediction of a Spike in Load

In order to better understand how well the predictive engine compensates for errors, consider a resistive load on a microgrid. Given a 480 V bus, a spike in power is generated with a base of 5 kW and a max of 15 kW by generating an inverse exponential representing resistance since $p = v^2/R$. To that end, let

$$\phi(t) = \begin{cases} a - b\mathrm{e}^{-t} & t \geq 0 \\ a - b\mathrm{e}^{t} & t < 0 \end{cases} \tag{4}$$

where

- $v = 480$ V
- $p_{\min} = 5000$ W
- $p_{\max} = 15000$ W
- $r_{\min} = \frac{v^2}{p_{\min}}$
- $r_{\max} = \frac{v^2}{p_{\max}}$
- $a = r_{\min}$
- $b = r_{\min} - r_{\max}$

The spike is shifted forward by 5 s. In order to model faulty or corrupted sensors, generated data is created with uniformly distributed random errors that vary between 0 and $\pm 2\ \Omega$ over a time interval that varies from 3 to 4.25 s. In all situations, 20 samples are collected. In order to match the curve to the data, Optizelle [7] is used and employs an inexact trust-region Newton algorithm. In all situations, the algorithm converged quickly and to a locally optimal solution.

Computationally, the accuracy of these predictions can be seen in Figures 4 and 5. Note that these predictions become more accurate as data is collected over a broader time period. Certainly, data collection over a smaller period can be tolerated, but it necessitates less error.

B. Differentiating Between Different Kinds of Loads

In the previous section, a spike in load with a known profile was considered. In the following experiment, this example is extended with two additional kinds of spikes. In addition to the inverse exponential, consider a quadratic spike in load of the form

$$\phi(t) = at^2 + bt + c \tag{5}$$

where

- $W = 5$
- $a = \frac{r_{\min} - r_{\max}}{W^2}$
- $b = 0\ \Omega$
- $c = r_{\max}$

and an oscillatory spike in load that follows a Ricker wavelet

$$\phi(t) = a + b\left(1 - \frac{t^2}{\sigma^2}\right)\mathrm{e}^{\frac{-t^2}{2\sigma^2}} \tag{6}$$

where

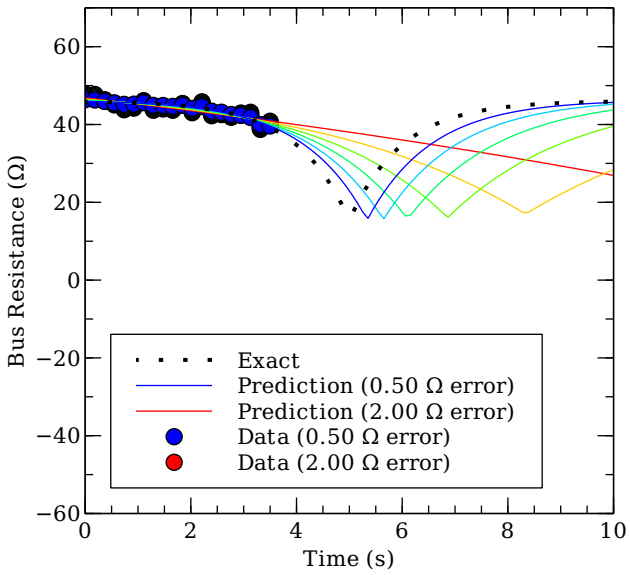

Fig. 4. Prediction of bus resistance following an inverse exponential with data between 0 and 3.5 s

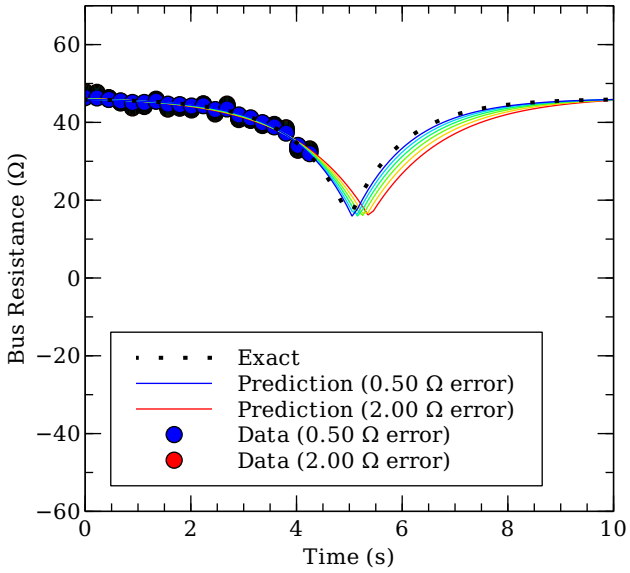

Fig. 5. Prediction of bus resistance following an inverse exponential with data between 0 and 4.25 s

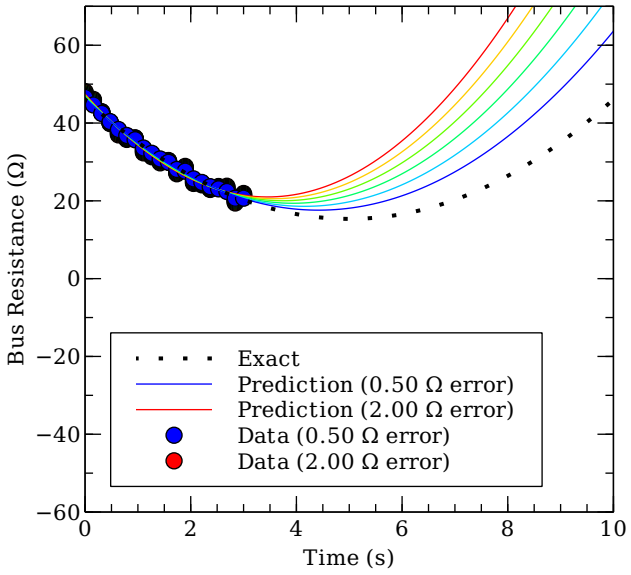

Fig. 6. Prediction of bus resistance following a quadratic with data between 0 and 3.0 s

- $\sigma = 1$
- $b = r_{\max} - r_{\min}$
- $a = r_{\min}$

The goal in this experiment is to determine how accurately the predictive engine can differentiate between different kinds of spikes in load under the same operating conditions in the preceding section. Namely, these experiments use the same amount of error and samples as before.

In the first case, the true load is set to follow a quadratic spike in load and the results are presented in Figures 6 and 7. Here, the quadratic load is correctly predicted in all situations. In the second case, the true load is set to follow the Ricker wavelet and the results are presented in Figures 8 and 9. In most situations, the predictive engine correctly identifies the type of load. However, when the time horizon is short and the error is high, there are a few situations where the predictive engine incorrectly predicts the load to be an inverse exponential. This reminds us of the limit of our predictive power when the amount of information is small.

C. Ship Microgrid Controller

In the final example, the impact of the predictive engine on the overall controller is considered. For this experiment, consider a reduced order model of an electric microgrid representing a ship in Figure 10, which is a variant of the configuration developed by Neely et al. [8]. Using the circuit components described in the introduction, and described in more detail by Wilson et al. [1], [2], this can be modeled with the components found in Figure 11. Notably, the port and starboard generators run at 120 V, but the port and starboard DC buses are required to remain between 220-260 V, and the central bus is required to remain between 450-500 V. In terms of currents, the generators are constrained to use no more that

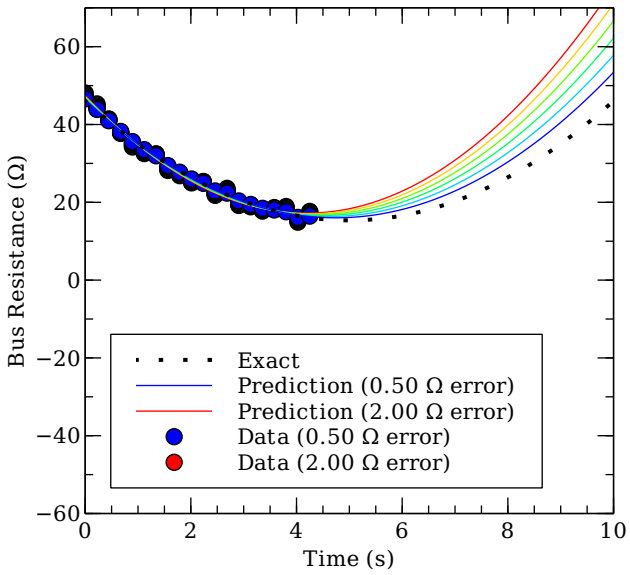

Fig. 7. Prediction of bus resistance following a quadratic with data between 0 and 4.25 s

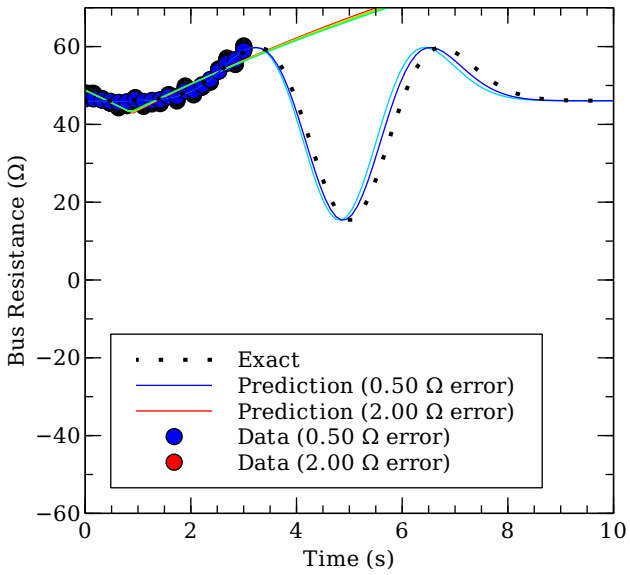

Fig. 8. Prediction of bus resistance following a Ricker wavelet with data between 0 and 3.0 s

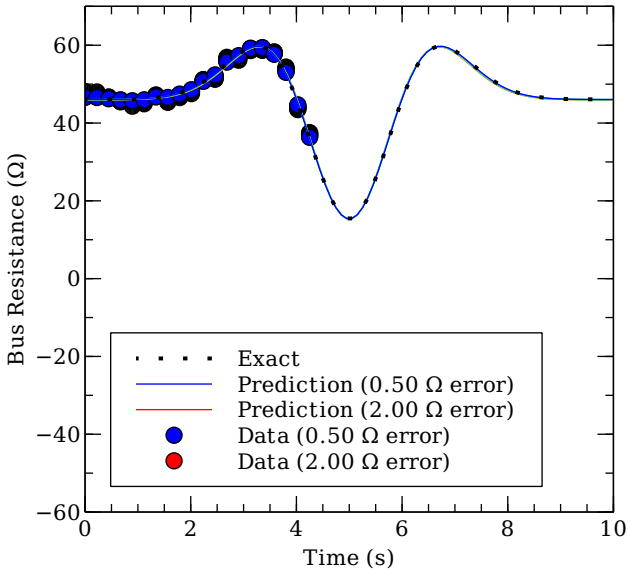

Fig. 9. Prediction of bus resistance following a Ricker wavelet with data between 0 and 4.25 s

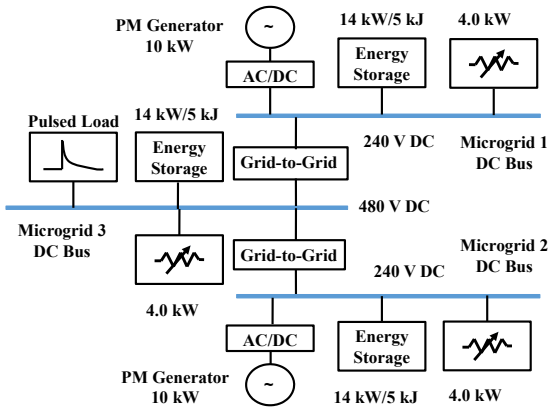

Fig. 10. Reduced order model of an electric microgrid representing a ship

83.3 A, which means they each produce 10,000 W at their maximum capacity. As far as the objective of the optimal control, the goal for this control is to satisfy the state equations for the grid while minimizing the use of storage devices. Finally, the control is solved for using Optizelle [7] configured to use an inexact composite-step SQP method combined with a primal-dual interior point method.

Before exercising the control, a spike in load is generated on the center microgrid and information about this event is collected over a 3 s time horizon. Then $\pm 0.50\ \Omega$ of uniformly distributed random error is added to the sensor readings. Based on this setup, the true load and prediction are given in Figure 12. Note, the prediction has about a 1 s delay in when it believes the peak of the spike in load to occur.

After solving for the control, the difference in the predicted resistive load with and without error can be seen in Figures 13 and 14. In short, the two computed loads differ by about

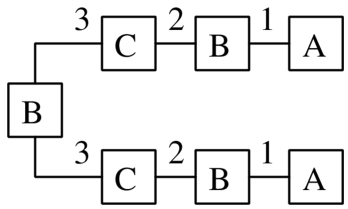

Fig. 11. Representation of the electric ship microgrid using the components described in Figures 1, 2, and 3

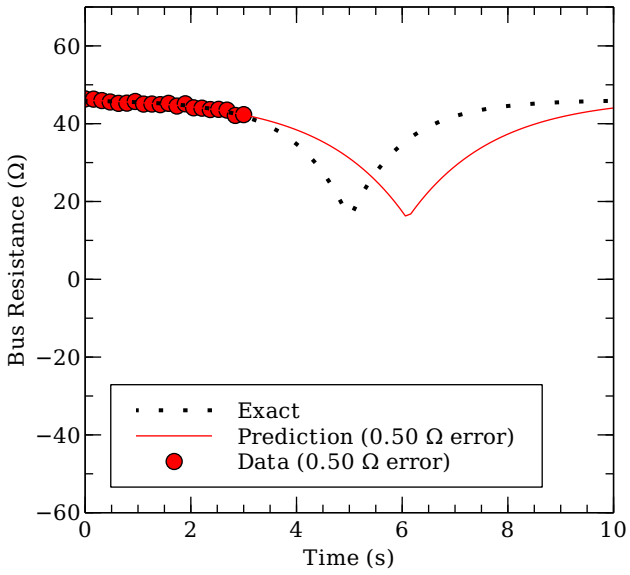

Fig. 12. True vs prediction of the spike in load on the center microgrid

1 s, which correlates with the error in the prediction. This leads to a predictable error in when the controller stores power demonstrated in Figures 15, 16, 17, and 18. However, in both cases, the controller always satisfy the voltage and current requirements described above in the problem setup. This can be seen in Figures 19, 20, 21, and 22.

In short, the controller was designed to never violate certain operating conditions such as those that specify valid ranges for the voltages and currents. These conditions remain valid even in the presence of sensor error. The error in the sensors gave rise to an inaccurate prediction in our load, which led to a delay in when the microgrid stored power. Certainly, a lower level controller may have had enough power to compensate for the actual operating conditions. Nonetheless, it can clearly be seen that error in the sensors leads to error in the prediction, which leads to error in the controller.

IV. Conclusions

This research presented details of the design and performance of a predictive engine integrated into an on-line optimal control planner for electrical microgrids. This discussion described how an on-line optimal control planner implements a receding-horizon control that relies on a predictive engine to predict the behavior of a system. Next, it was shown

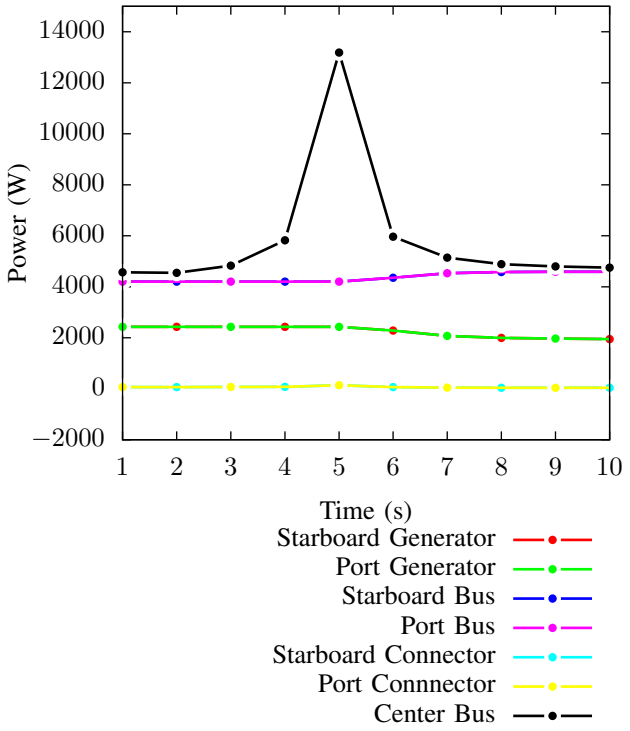

Fig. 13. Computed resistive load with exact prediction

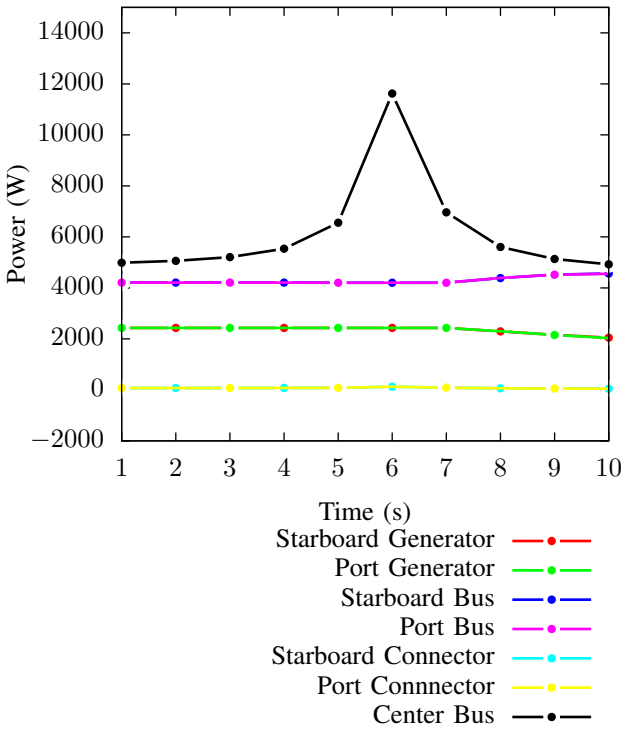

Fig. 14. Computed resistive load with error in prediction

how to produce a predictive engine for the kinds of loads seen in a microgrid. In the computational examples, it was observed that one could accurately predict a spike in load given a limited amount of information with error. Further, it was shown that the predictive engine could also differentiate between different kinds of spikes in load as long as sufficient information was available with high enough accuracy. Finally, it was demonstrated how this predictive engine integrates directly into an optimal control algorithm used to manage the power on an electric ship. Here, it was seen that the performance of the microgrid depends directly on the accuracy of the predictive engine. Although the controller incurred error in calculating when power should be stored and distributed, the controller never violated the specified operating conditions.

In the future, this work can be extended to provide predictions for higher-dimensional data and assess the impact of these predictions on the control infrastructure. In addition, there's an interaction between the predictive engine, the controller, and an additional energy management layer that coordinates between the two. Ultimately, this energy management layer must decide when a prediction is adequate and when the control's performance has deviated too far from the optimal control. This layer needs additional analysis to determine best practices for improving the overall performance of the system.

ACKNOWLEDGMENT

The authors would like to acknowledge our NAVSEA Naval Power Systems, Electric Ship PMS 320 program for their support. Sandia National Laboratories is a multimission laboratory managed and operated by National Technology and Engineering Solutions of Sandia, LLC., a wholly owned

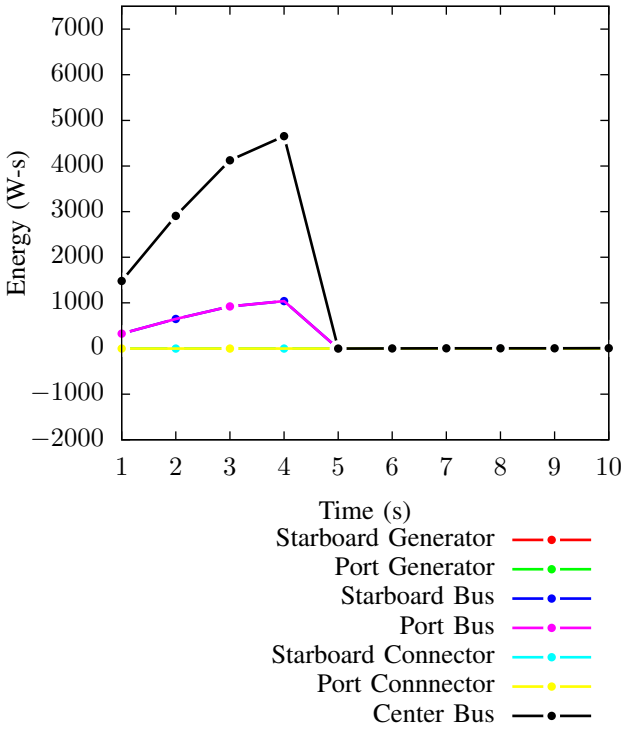

Fig. 15. Energy in storage with exact prediction

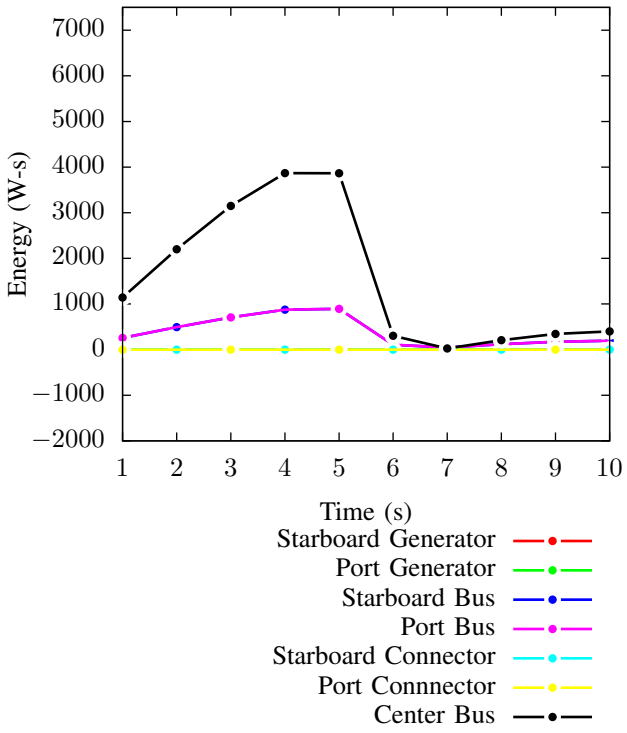

Fig. 16. Energy in storage with error in prediction

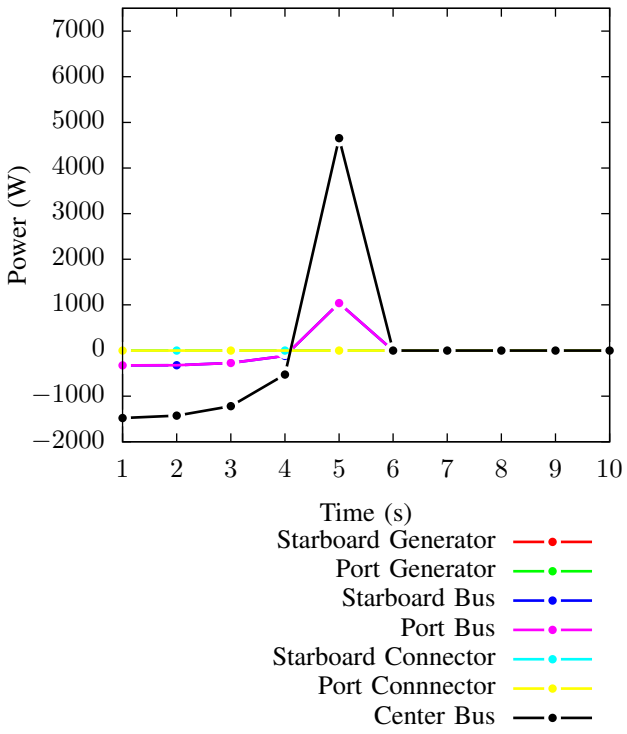

Fig. 17. Power from storage with exact prediction

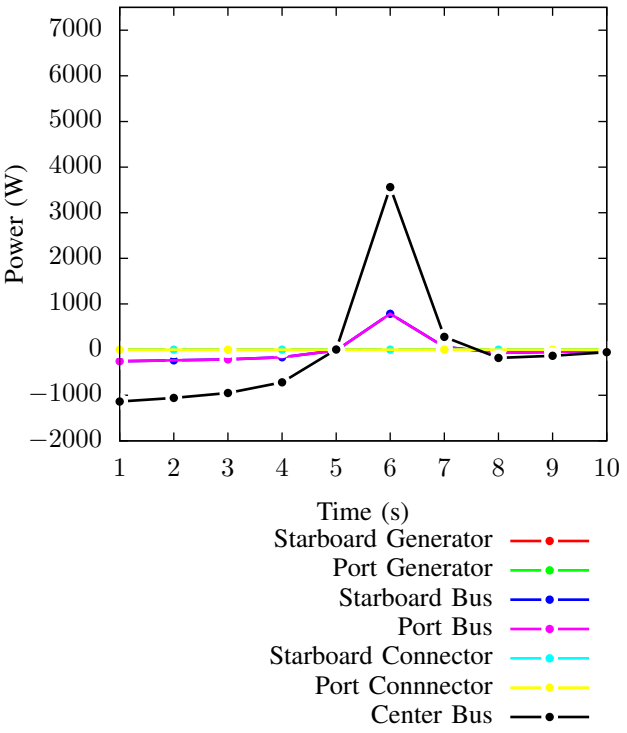

Fig. 18. Power from storage with error in prediction

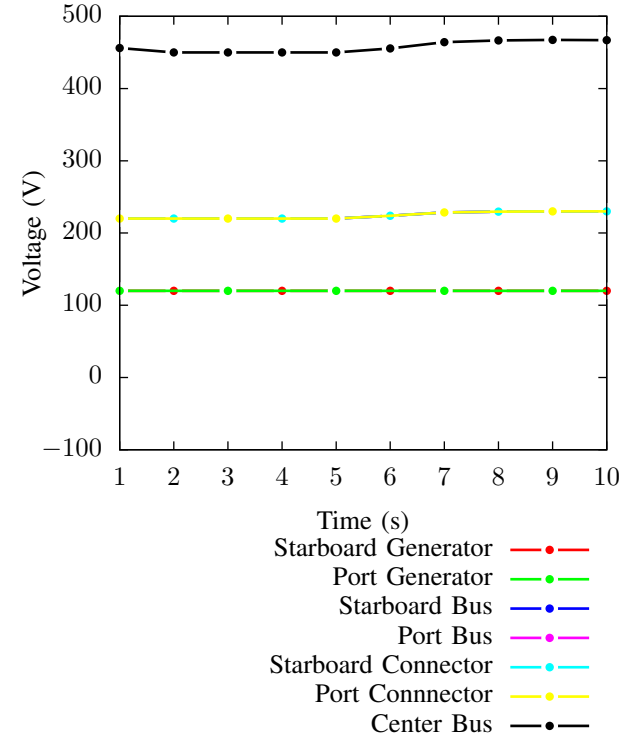

Fig. 19. Voltage with exact prediction

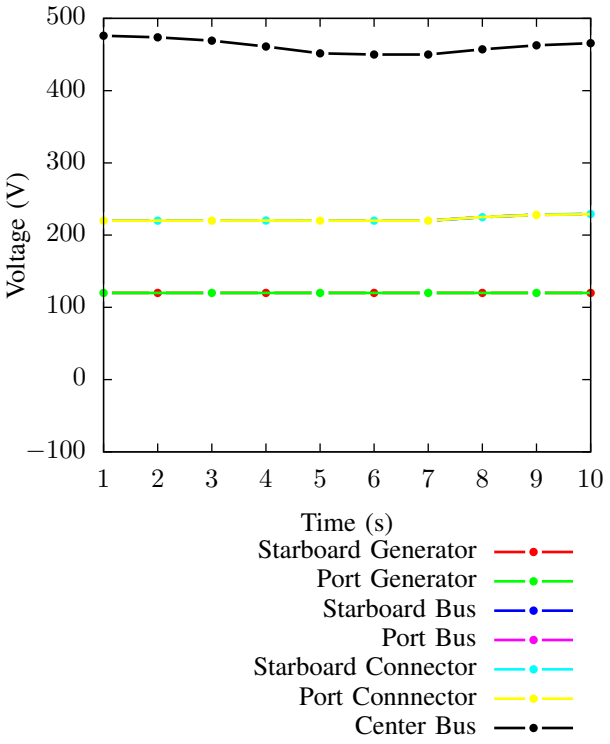

Fig. 20. Voltage with error in prediction

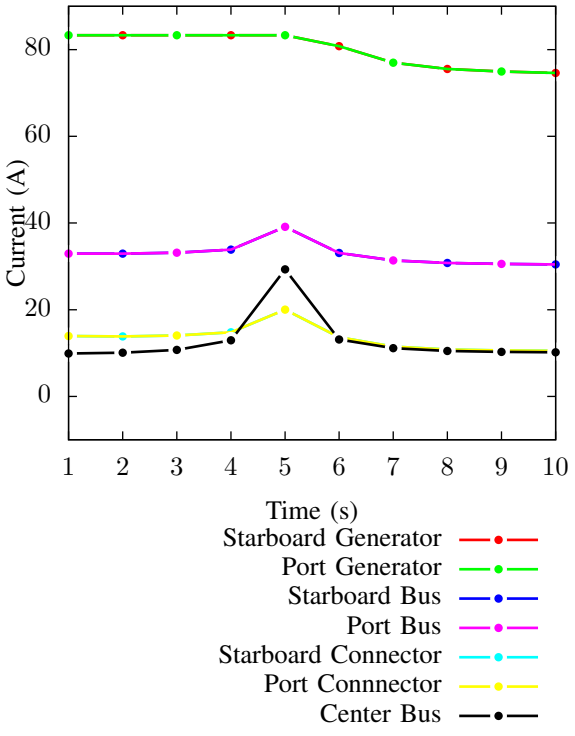

Fig. 21. Current with exact prediction

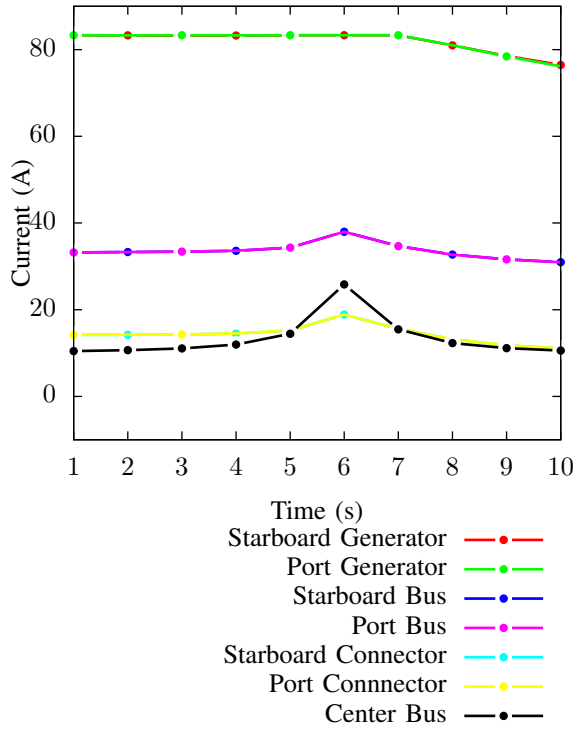

Fig. 22. Current with error in prediction

subsidiary of Honeywell International, Inc., for the U.S. Department of Energy's National Nuclear Security Administration under contract DE-NA0003525.

REFERENCES

[1] D. G. Wilson, J. C. Neely, M. A. Cook, S. F. Glover, J. Young, and R. D. Robinett, "Hamiltonian control design for dc microgrids with stochastic sources and loads with applications," in *2014 International Symposium on Power Electronics, Electrical Drives, Automation and Motion*, June 2014, pp. 1264–1271.

[2] D. G. Wilson, R. D. Robinett, W. W. Weaver, R. H. Byrne, and J. Young, "Nonlinear power flow control design of high penetration renewable sources for ac inverter based microgrids," in *2016 International Symposium on Power Electronics, Electrical Drives, Automation and Motion (SPEEDAM)*, June 2016, pp. 701–708.

[3] S.-S. Jang, B. Joseph, and H. Mukai, "On-line optimization of constrained multivariable chemical processes," *AIChE Journal*, vol. 33, no. 1, pp. 26–35, 1987.

[4] L. T. Biegler, "Efficient solution of dynamic optimization and nmpc problems," in *Nonlinear Model Predictive Control*, F. Allgwer and A. Zheng, Eds. Springer Basel AG, 2000, pp. 219–243.

[5] H. Park, J. Sun, S. Pekarek, P. Stone, D. Opila, R. Meyer, I. Kolmanovsky, and R. DeCarlo, "Real-time model predictive control for shipboard power management using the ipa-sqp approach," *IEEE Transactions on Control Systems Technology*, vol. 23, no. 6, pp. 2129–2143, Nov 2015.

[6] R. Ghaemi, J. Sun, and I. V. Kolmanovsky, "An integrated perturbation analysis and sequential quadratic programming approach for model predictive control," *Automatica*, vol. 45, no. 10, pp. 2412 – 2418, 2009.

[7] J. Young, "Optizelle – an open source software library designed to solve general purpose nonlinear optimization problems," www.optimojoe.com, 2013–2017.

[8] J. Neely, L. Rashkin, M. Cook, D. Wilson, and S. Glover, "Evaluation of power flow control for an all-electric warship power system with pulsed load applications," in *2016 IEEE Applied Power Electronics Conference and Exposition (APEC)*, March 2016, pp. 3537–3544.